

Silicon Nanoparticles Produced by Femtosecond Laser Ablation

Nikolaos G. SEMALTIANOS, Walter PERRIE, Stuart P. EDWARDSON, Geoff DEARDEN,

Martin SHARP and Ken G. WATKINS

Lairdside Laser Engineering Centre, University of Liverpool, Campbelltown Road, Wirral CH41 9HP, U.K.

E-mail: n.semaltianos@liverpool.ac.uk

Femtosecond laser ablation of solids usually carried out in vacuum or liquid environments, offers a novel and reliable method for the production of nanoparticles of different materials. In this work we have investigated the production of nanoparticles by femtosecond laser ablation (775 nm, 180 fs, 1 kHz, fluence: 0.05-1.6 J cm⁻²) of the target material in air. We focus mainly on silicon nanoparticles and use Atomic Force Microscopy, Transmission Electron Microscopy and Energy Dispersive X-ray Analysis. Si nanoparticles produced in air are single crystals with an average height distribution of 40-50 nm in areas where the debris is in the form of a continuous deposit, and 9-11 nm in areas where the debris is in the form of isolated particles. This is comparable to the average size distribution of 6-12 nm of particles produced previously in vacuum. The nanoparticles have disk shape with long to short axis length ratio in the region 7-10 which is larger than the eccentricity of 1.4-6.6 found previously for silicon nanoparticles produced in vacuum.

Keywords: Nanoparticles, laser ablation, femtosecond, silicon, atomic force microscopy, transmission electron microscopy

1. Introduction

There is an increasing interest in the production and characterization of nanoparticles (NPs) of different elements and compounds due to their importance in fundamental research as well as in technological applications [1]. Different techniques for the production of NPs have been used, such as arc discharge, vapour and electrochemical deposition, ball milling, sputtering and laser ablation with long nanosecond pulses. Recently femtosecond laser ablation of solid targets either in vacuum or liquid environment has been suggested and used as a powerful and versatile method for the production of metal and semiconductor NPs, simply due to the facts that femtosecond pulses do not interact with the ejected particles (the pulse ends before the plume expansion starts) thus avoiding complicated secondary laser-material interactions, a supercritical material is created at solid state density and also because the stoichiometry of the original target is maintained in the produced particles [2-4].

In this work we have investigated, by using Atomic Force Microscopy (AFM), Transmission Electron Microscopy (TEM) and Energy Dispersive X-ray Analysis (EDX), Si NPs produced by femtosecond laser ablation of the target in air.

2. Experimental Details

A Clarke-MXR CPA-2010 femtosecond laser system was used for the ablation. It delivers ~1mJ per pulse at 1 kHz rep. rate and $\lambda=775$ nm, 180 fs pulselength and observed bandwidth $\Delta\lambda\sim 5.5$ nm. The output is attenuated before being directed to the input aperture of a scanning galvo with 100mm focal length f- θ lens. The spot size $2\omega_0$ ($1/e^2$) diameter at the focal plane was measured to be ~ 50

μm . The substrates were mounted horizontally and the substrate surface could be brought to the focal plane using a precision vertical lab jack with 10 μm resolution. For generation of nano-particle debris, percussion drilling was performed near normal incidence on the substrate with N = 100 pulses and with pulse energies from 1 to 30 μJ (fluence ~ 0.05-1.5 J cm⁻²). AFM imaging was performed on the debris produced around the ablated region with a Veeco CP-II instrument in non-contact mode using Si cantilevers with radius of curvature less than 10 nm (Tap300). For TEM measurements the debris was collected on a carbon coated grid which was placed at a distance of ~ 30 μm from the centre of the ablated hole. TEM was performed with a JEOL JEM-2000FXII instrument equipped with EDS Genesis 4000 system to enable also acquisition of EDX spectra.

3. Results and discussions

Fig. 1 shows an optical microscope picture taken under side white light illumination, of a crater machined (percussion drilling) on a silicon substrate with 100 pulses at a fluence of 1.6 J cm⁻². The debris spreads around the ablated area in a circle with a well defined diameter of ~ 300 μm . Around the perimeter of the circle, a ring with thickness of ~10 μm is observed.

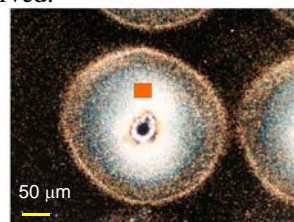


Fig. 1 Debris spreading around a hole made by laser ablation of Si in air.

Systematic measurements of the debris spreading diameter versus pulse energy are plotted in Fig. 2. A minimum debris spreading diameter of $\sim 32 \mu\text{m}$ is observed for fluence of 0.05 J cm^{-2} . The inset in Fig. 2 shows that the debris diameter follows a linear behaviour with laser pulse energy in log-log scale as expected by the Sedov-Taylor theory for shock wave expansion [5].

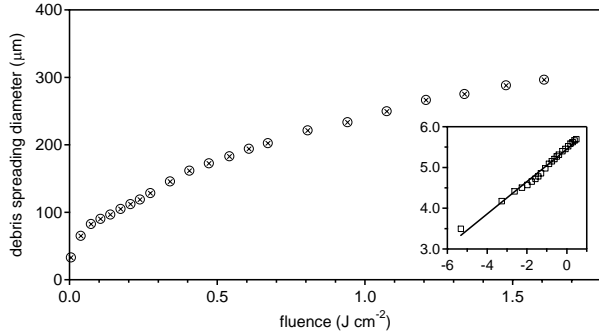


Fig. 2 Debris spreading diameter versus laser fluence. Inset shows linear behaviour in log-log scale.

To get information about the microscopic properties of the debris following the laser ablation, we have scanned by AFM a region around the ablated crater where the debris is formed. An AFM image taken in non-contact mode of the debris on the area marked by the orange rectangle in Fig. 1, where a continuous deposit is formed, is shown in Fig. 3 (Fig. 4 shows a 3-D view of the image), on a sample ablated with 100 pulses at laser fluence of $\sim 0.104 \text{ J cm}^{-2}$.

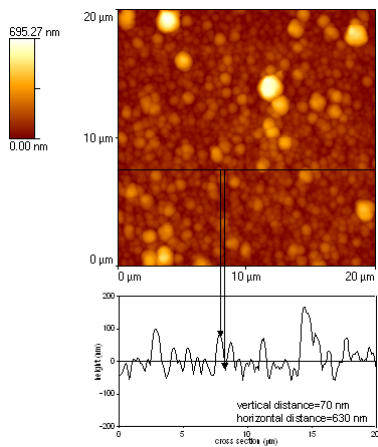


Fig. 3 AFM image of Si NPs and cross sectional graph.

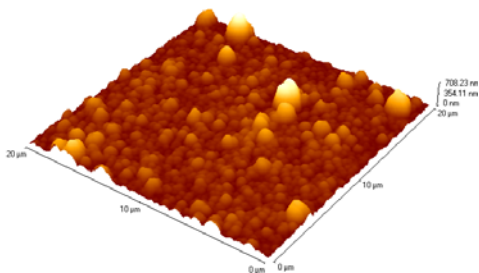


Fig. 4 3-D view of the image in Fig. 3.

It is seen that the debris consists of nanoparticles with an average height of $\sim 40\text{-}50 \text{ nm}$ as it is seen from the histogram of Fig. 5 (a) (percentage of particles with a certain height). Fig. 5 (b) shows the bearing ratio of the image denoting the percentage of the image with a certain height. It is seen for instance that no more than $\sim 20 \%$ of the image has height above $\sim 145 \text{ nm}$ (marked by green).

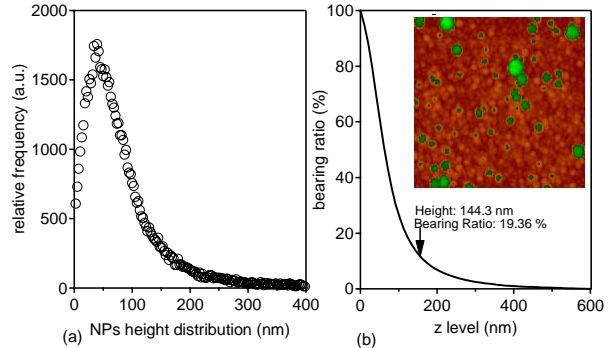


Fig. 5 Height histogram of the continuous deposits showing particle height distribution (a), and bearing ratio plot showing percentage of the image with height below a certain level.

Fig. 6 shows AFM images of the area outside of the debris ring (distance $>30 \mu\text{m}$), where the debris is in the form of isolated particles.

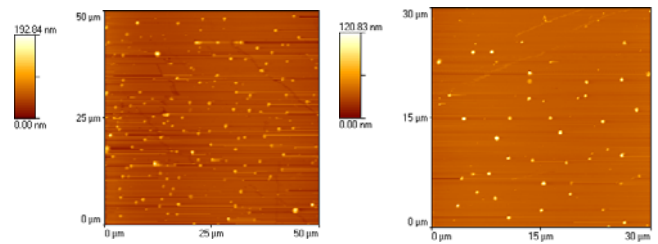


Fig. 6 AFM images of Si NPs on the area of the substrate where the debris appears as isolated particles.

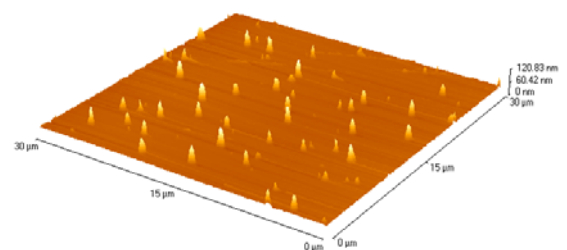
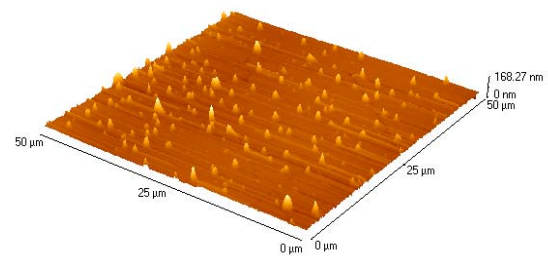


Fig. 7 3-D views of the images in Fig. 6.

From the height histogram (Fig. 8) it is seen that the nanoparticles have an average height of ~9-11 nm. Bearing ratio shows that no more than ~10 % of the surface has height above 20 nm.

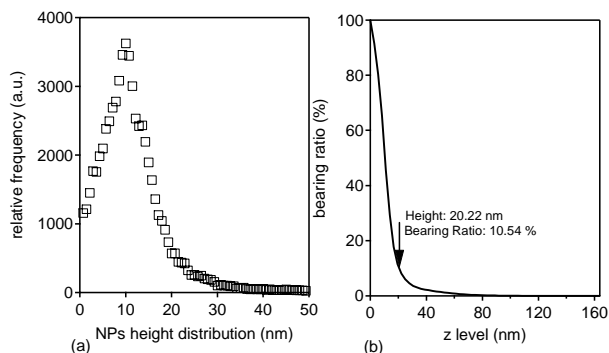


Fig. 8. Height histogram of isolated particles deposits showing particle height distribution (a), and bearing ratio plot showing percentage of the image with height below a certain level (b).

The average height of Si nanoparticles in sub-monolayer coverage which are made here by femtosecond laser ablation of the target in air, is comparable to the average size of Si nanoparticles which were made by ablation in high vacuum of the order of 10^{-7} mbar and which have sizes between 6-12 nm for laser fluences in the region 0.3-1.2 J/cm² [4,5]. This is also smaller than the size of silicon nanoparticles produced by ablation with a 510.5 nm, 20 ns, 15 kHz laser pulses in liquid environments (water, dichloroethane or ethanol) which have been found to have sizes ranging from 60-90 nm for laser fluences in the range of 0.7-1.5 J/cm² and also has been shown to be polycrystalline [6].

An interesting characteristic of the silicon nanoparticles is that they in fact have disk shape with the plane of the disk parallel to the substrate surface. This can be seen for example from the cross sectional graph of Fig. 3 where the major and minor axes of the disk have been measured on the image (ratio ~9). The disk shape of silicon nanoparticles has already been observed also in the case of vacuum ablation (pressure $\leq 10^{-5}$ Pa) with 0.85 ps/1055 nm or 0.30 ps/527 nm laser pulses and intensities in the range of 2.9×10^{11} - 3.7×10^{12} W/cm² and ratio of axes in the region of 1.4-6.6 [7].

TEM images of the debris collected on a carbon coated grid is shown in Fig. 9. The nanoparticles are single crystals with d spacing of the $\sim 1.71 \pm 0.08$ Å (corresponding to {311}) which is confirmed by the electron diffraction pattern as shown in Fig. 9. EDX spectra shows that the NPs consist mainly of silicon with a small percentage of oxygen.

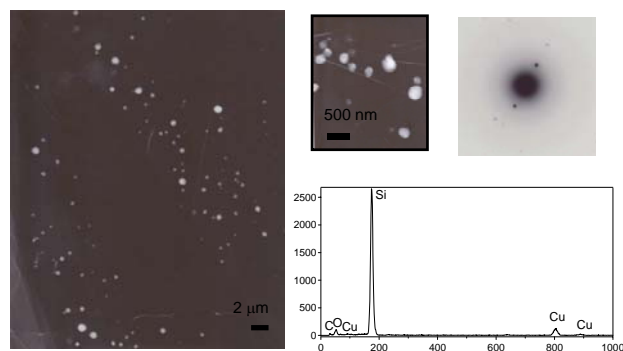


Fig. 9 TEM images of silicon nanoparticles produced by laser ablation in air. X-Ray diffraction pattern confirming crystalline structure of particles. EDX spectrum.

4. Conclusions

In addition to the well established method for the production of nanoparticles by femtosecond laser ablation of the target material in vacuum or liquid environments, nanoparticles of at least Si can be produced by femtosecond laser ablation of the target material also in air. The particles have disk shapes and average height comparable to the size of those produced in vacuum.

Acknowledgments

The authors acknowledge support by the European Community and NWDA U.K.

References

- [1] S. A. Edelstein and R. C. Cammarata: "Nanomaterials: Synthesis, Properties and Applications" (Publisher: Institute of Physics, 1996).
- [2] A. V. Simakin, V. V. Woronov, N. A. Kirichenko and G. A. Shafeev: *Appl. Phys. A*, 79, (2004) 1127.
- [3] S. Eliezer, N. Eliaz, E. Grossman, D. Fisher, I. Gouzman, Z. Henis, S. Pecker, Y. Horovitz, M. Fraenkel, S. Maman and Y. Lereah: *Phys. Rev. B*, 60, (2004) 144119.
- [4] S. Amoroso, G. Ausanio, R. Bruzzese, M. Vitiello and X. Wang: *Phys. Rev. B*, 71, (2005) 033406.
- [5] T. E. Glover: *J. Opt. Soc. Am. B*, 20, (2003) 125.
- [6] Y. B. Zel'dovich and Y. P. Raizer: *Physics of Shock Waves and High Temperature Hydrodynamic Phenomena* (academic, New York, 1966).
- [7] S. I. Dolgaev, A. V. Simakin, V. V. Voronov, G. A. Shafeev and F. Bozon-Verduraz: *Appl. Surf. Science*, 186, (2002) 546.
- [8] G. Ausanio, S. Amoroso, A. C. Barone, R. Bruzzese, V. Iannotti, L. Lanotte and M. Vitiello: *Appl. Surf. Science*, 252, (2006) 4678.